Femtosecond-laser-induced reversal in in-plane-magnetized spin valves

Jun-Xiao Lin, Yann Le Guen, Julius Hohlfeld, Junta Igarashi, Quentin Remy, Jon Gorchon, Grégory Malinowski, Stéphane Mangin, Thomas Hauet, Michel Hehn

Femto-second Laser Induced Reversal in In-Plane Magnetized Spin Valves

Jun-Xiao Lin,[1] Yann Le Guen,[1] Julius Hohlfeld,[1] Junta Igarashi,[1] Quentin Remy,[2] Jon Gorchon,[1] Grégory Malinowski,[1] Stéphane Mangin,[1,3] Thomas Hauet[1] and Michel Hehn*[1,3]

[1]*Université de Lorraine, CNRS, Institut Jean Lamour, F-54000 Nancy, France*

[2]*Department of Physics, Freie Universität Berlin, 14195 Berlin, Germany*

[3]*Center for Science and Innovation in Spintronics, Tohoku University, Sendai, Japan*

*Authors to whom correspondence should be addressed: michel.hehn@univ-lorraine.fr

Abstract

Ultrashort spin-polarized electron pulses, generated through optically driven ultrafast demagnetization, have demonstrated high efficiency in achieving magnetization reversal of a ferromagnetic layer within a few hundred femtoseconds. Previous studies have focused on magnetization reversal in perpendicularly magnetized spin valves, where the static magnetization configuration and its dynamics are strongly influenced by the substantial demagnetization field inherent in this geometry. Consequently, the impact of layer thickness on the reversal process in such configurations presents a significant challenge and has been rarely studied. Here, we investigate in-plane magnetized GdCo/Cu/ferromagnetic layer spin valves to isolate the impact of the Curie temperature and the ferromagnetic layer thickness on magnetization switching. We demonstrate that the threshold laser fluence necessary for reversing the ferromagnetic layer increases with the Curie temperature and the ferromagnetic layer thickness. Additionally, our findings indicate that achieving complete reversal may require multiple pulses, with the number of pulses needed increasing with the Curie temperature and the thickness of the ferromagnetic layer. The maximum thickness of the ferromagnetic layer that allows for full reversal is limited by the Gd concentration in the GdCo spin current source layer. These results enhance our understanding of ultrafast magnetization reversal induced by ultrafast spin pumping and offer valuable insights for designing energy-efficient magnetic memory devices.

I. INTRODUCTION

The incorporation of ultrafast optical magnetization control into spintronic devices offers a promising energy-efficient approach for magnetic random-access memory (MRAM) design [1-4]. This benefit arises from the rapid reduction of magnetic order driven by femtosecond laser excitation-induced heating, a phenomenon known as ultrafast demagnetization [5]. This ultrafast demagnetization, in metallic magnetic materials, generates ultrashort spin-polarized current pulses [6-9], a phenomenon referred to as ultrafast spin pumping [4,8]. This non-local angular momentum transfer [10-13], has been shown to induce ultrafast magnetization reversal [14-16]. In a single ferrimagnetic layer such as GdCo and MnRuGa, the angular momentum transfer between two antiferromagnetically exchange-coupled magnetization sublattices leads to sub-picosecond single pulse magnetization reversal in both perpendicular magnetized [17-20] and in-plane magnetized [21] samples. In a spin valve architecture, there is a capability to decouple the spin current pulse source from the layer impacted by the spin current. This capability was initially demonstrated in an experiment exploring single pulse reversal of a ferromagnetic layer [22]. The study used a collinear spin valve structure composed of GdFeCo/Cu/[Co/Pt] with perpendicular magnetic anisotropy. The final orientation of [Co/Pt] magnetization is determined by the spin currents generated from the Gd sublattices within GdFeCo [23]. Precise control of ultrafast demagnetization in both the GdFeCo and the ferromagnetic layer is required to achieve efficient magnetization switching. It has been demonstrated that the amount of laser fluence required to reverse the ferromagnetic layer depends on the Gd content in GdFeCo [24] and that the ability of the ferromagnetic layer to be switched by the Gd spin current depends on its Curie temperature [25]. The latter demonstrates that the remaining magnetization in the ferromagnetic layer needs to be sufficiently low to ensure its switching upon interaction with the Gd spin current. Gd is believed to provide a higher spin current intensity compared to other magnetic materials [4,23,26]. However, in 2023, Igarashi *et al.* demonstrated single pulse switching in Gd-free archetypal spin valves comprising [Co/Pt]/Cu/[Co/Pt] [16]. The combination of ultrafast spin pumping and ultrafast demagnetization has enabled the achievement of unprecedented reversal times on the order of a few hundreds of femtoseconds [4,16].

In this study, we first demonstrate magnetization switching in in-plane magnetized ferromagnetic (FM) layers integrated in a spin-valve architecture using multiple femtosecond pulses. In this geometry, we do not have to consider the presence of a strong demagnetization field; the FM layer does not require heavy elements to ensure a perpendicular anisotropy, and its thickness can be much larger than in the perpendicular geometry. The model systems studied

are GdCo/Cu/FM in-plane magnetized spin valves, using CoNi and CoFeB alloys to investigate the effect of the Curie temperature. In these cases, we demonstrate that increasing the Curie temperature of the FM layer leads to an increase in both the number of pulses and the pulse fluence required for reversal. Additionally, we show that reducing the FM layer thickness while maintaining its Curie temperature decreases the number of pulses and the amount of spin current needed for switching. We observed a transition from multiple to single current pulse-induced full reversal by reducing the thickness of the CoFeB FM layer from 3 to 1 nm and confirmed the importance of ensuring sufficient demagnetization of the FM layer upon interaction with enough spin current. Moreover, we revealed that lowering the Gd concentration in the GdCo spin current source layer decreases the maximum thickness limit at which full reversal of the FM layer can be observed.

II. EXPERIMENTAL SECTION/METHODS

A. Sample preparations

All in-plane magnetized spin valve structures were prepared using DC/RF magnetron co-sputtering with elemental targets and processed under an Argon gas pressure of around 10^{-3} mbar. The multilayered structures were deposited onto 15×10-mm glass substrates at room temperature, with a deliberate effort to ensure that the layer deposition was conducted in the stray field of the magnetron gun by sweeping the sample over both targets. This process results in a well-defined in-plane anisotropy [21]. Two series of heterostructures used in this study are presented as follows:

(1) The first series: Glass/Ta (3 nm)/Co (3 nm)/$Gd_{33}Co_{67}$ (5 nm)/Cu (10 nm)/FM (3 nm)/Pt (3 nm), where FM represents a ferromagnetic layer. The FM layers include Co_xNi_{100-x} alloys with concentrations of x=10%, 20%, and 40%, and $Co_{40}Fe_{40}B_{20}$.

(2) The second series: Glass/Ta (3 nm)/Gd_yCo_{100-y} (5 nm)/Cu (5 nm)/$Co_{40}Fe_{40}B_{20}$ (t nm)/Pt (3 nm), where the thickness t of the CoFeB layers ranges from 1 nm up to 2.45 nm, and the Gd concentration y is either 25% (Gd-rich) or 17.5% (Co-rich).

Note that the compensation composition was identified as y=21% in all these samples, and the GdCo/Cu/FM spin valves have the same interfaces.

B. All-optical switching static measurement

Hysteresis loops and static single pulse measurements were conducted using a longitudinal magneto-optic Kerr effect (MOKE) configuration at room temperature. In this

setup, both laser pump and probe beams were directed onto the side of the ferromagnetic layers. For the static single pulse measurements, an external in-plane magnetic field (oriented parallel to the substrate and along the in-plane easy axis) with a strength greater than the sample coercivity was initially applied to initialize the sample. This process ensured that all magnetic moments in the sample were aligned in the direction of the in-plane easy axis once the field was turned off. Subsequently, the samples were irradiated by different numbers of laser pulses without applying any external magnetic field to perform the all-optical switching measurements. In the MOKE microscope setup utilized in this study, a complementary metal oxide semiconductor camera captured a single image of magnetic domains. The camera boasted a resolution of 1920×1080 pixels, with each pixel measuring approximately 5 μm.

III. RESULTS

A. Experiments

Two types of in-plane spin valve structures were characterized and fabricated. Glass/Ta (3 nm)/Co (3 nm)/$Gd_{33}Co_{67}$ (5 nm)/Cu (10 nm)/FM (3 nm)/Pt (3 nm), where FM stands for a ferromagnetic layer, is the first one. Four different FM layers, including Co_xNi_{100-x} alloys with concentrations of x=10%, 20%, and 40%, as well as $Co_{40}Fe_{40}B_{20}$, were selected to investigate the impact of the FM's Curie temperature (T_C) on the magnetization switching. The ferrimagnetic $Gd_{33}Co_{67}$ layer was chosen as a source of spin current with a Gd concentration of 33% to maximize spin angular momentum from the Gd sublattice [24]. Note that a thick ferromagnetic Co (3 nm) layer is exchange coupled to the $Gd_{33}Co_{67}$ layer to pin the latter in a given direction in order to permit multiple pulses experiments [4]. The second sample series Glass/Ta (3 nm)/Gd_yCo_{100-y} (5 nm)/Cu (5 nm)/$Co_{40}Fe_{40}B_{20}$ (t nm)/Pt (3 nm) is made to study the CoFeB switching efficiency, at constant T_C, as a function of the thickness t, ranging from 1 nm up to 2.45 nm, and as a function of the spin current from Gd sublattice. The spin current source is given by the Gd concentration (y), being either 25% (Gd-rich) or 17.5% (Co-rich). Detailed descriptions of the sample preparation are provided in the EXPERIMENTAL SECTION/METHODS.

To perform all-optical switching experiments, a linearly polarized pump laser pulse with a wavelength of 1030 nm and a pulse length of 250 fs is directed perpendicularly to the film plane. The linearly *p*-polarized probe beam, with a wavelength of 515 nm, is incident at an angle of 45° (Fig. 1(a)). In this experimental setup, both the pump and probe beams illuminate the FM layer side of the sample.

B. Variation of the Curie temperature for ferromagnetic layers with a fixed thickness

Fig. 1 presents the Co (3 nm)/$Gd_{33}Co_{67}$ (5 nm)/Cu (10 nm)/FM (3 nm) spin-valves and their magnetic properties. The $Gd_{33}Co_{67}$ layer is a Gd-rich alloy, meaning that the net magnetization of $Gd_{33}Co_{67}$ is parallel to the magnetization of the Gd sublattice. Nevertheless, the total magnetic moment of the Co (3 nm)/$Gd_{33}Co_{67}$ (5 nm) bilayer is dominated by the Co, resulting in the net magnetization aligning with the magnetization of the Co sublattice. Fig. 1(b) summarizes the Curie temperature (T_C) values for the four tested FM (three CoNi and one CoFeB alloy) measured by a commercial superconducting quantum interference device (SQUID). As expected from the T_C of pure Co, around 1300 K, and pure Ni, around 600 K, the T_C of the Co_xNi_{100-x} layer rises when the Co concentration increases. The T_C value of $Co_{40}Fe_{40}B_{20}$ falls within the range of T_C values observed for Co_xNi_{100-x} alloy concentrations ranging from 20% to 40%. Previous reports suggest that the T_C of $Gd_{33}Co_{67}$ is approximately 600 K [27,28], which corresponds to the T_C values observed for Co_xNi_{100-x} alloy concentrations ranging from 10% to 20%. Fig. 1(c) and 1(d) display the longitudinal magneto-optic Kerr effect (MOKE) signal (θ_K) as a function of the magnetic field applied along the in-plane easy axis direction for two spin valves, one including $Co_{20}Ni_{80}$ and the other one CoFeB, respectively. The coercivity of the FM layer is smaller than that of Co (3 nm)/$Gd_{33}Co_{67}$ (5 nm). Consequently, these spin valves allow access to four distinct magnetic configurations (P^+, AP^-, P^-, AP^+). The parallel configurations (P^+ or P^-) designate the state where the magnetization of the transitional metal sublattice in the Co/$Gd_{33}Co_{67}$ aligns parallel with that of the FM layer. On the other hand, the antiparallel configurations (AP^+ or AP^-) correspond to the state where the Co moments in the Co/$Gd_{33}Co_{67}$ are antiparallel to that of the FM layer. The magnetic configurations are labeled positive (P^+ or AP^+) or negative (P^- or AP^-) based on whether the magnetization in the FM layer aligns with the positive or negative field direction, respectively. Table 1 shows the four accessible magnetic configurations of the magnetic spin valve structure ((Co)/GdCo/Cu/FM), which are consistently referenced throughout this article. The absence of a noticeable field shift of the FM layer minor loop suggests the absence of coupling between the FM and the Co/$Gd_{33}Co_{67}$ layers. Note that the CoFeB-based spin valve exhibits a squarer-shaped hysteresis loop compared to that with CoNi. Indeed, the polycrystalline nature of the Co_xNi_{100-x} layer results in non-uniform local magnetization directions with small fluctuations known as magnetization ripple when the thickness is less than the grain size [29,30]. Below this critical threshold, which we have found to be about 3 nm, the uniaxial in-plane anisotropy

weakens, causing a reduction in remanence. In contrast, CoFeB exhibits an amorphous nature that does not suffer the appearance of magnetization ripple, even at reduced thicknesses.

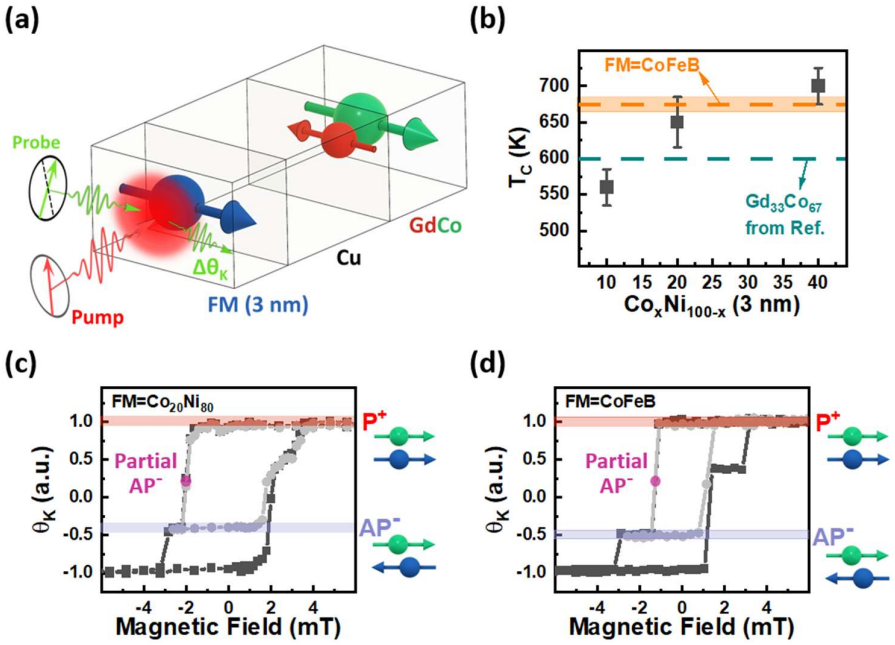

FIG. 1. Magnetic properties of Co (3 nm)/Gd-rich $Gd_{33}Co_{67}$ (5 nm)/Cu (10 nm)/ferromagnetic (FM) layer (3 nm) spin valves. (a) Schematic of the multilayer stack with the FM layer being either $Co_{10}Ni_{90}$, $Co_{20}Ni_{80}$, $Co_{40}Ni_{60}$, or $Co_{40}Fe_{40}B_{20}$, and the laser pump-probe geometry. The blue three-dimensional arrow represents the magnetization in the FM layer, while the red and green arrows denote the magnetizations of Gd and Co in the Co/GdCo layer, respectively. The pump laser pulse, linearly polarized at 1030 nm and a pulse duration of 250 fs, is directed perpendicular to the film plane. The linearly *p*-polarized probe beam at 515 nm is incident at a 45° angle. The pump pulse has a diameter of approximately 180 μm and a fixed repetition rate of 100 kHz. Both the pump and probe beams illuminate the FM layer side. (b) The Curie temperature (T_C) of various magnetic layers is measured using a superconducting quantum interference device (SQUID). The square-filled dots indicate the T_C of different Co_xNi_{100-x} (3 nm) alloys plotted as a function of Co concentration x. The orange dashed line represents the T_C for $Co_{40}Fe_{40}B_{20}$ (3 nm), with the semi-transparent orange region denoting the error bar for its T_C. Additionally, the dark cyan dashed line corresponds to the T_C for the $Gd_{33}Co_{67}$ alloy, obtained from references [27,28]. Normalized longitudinal Kerr hysteresis loops are presented for the spin valve, with (c) $Co_{20}Ni_{80}$ and (d) CoFeB as the FM layer.

Table 1. The four possible magnetic configurations, illustrating the relative directions of the magnetic moments of different magnetic elements. Note that this table only presents the relative magnetic moment directions between the elements; the individual magnetization magnitudes of each element are not considered.

Denotation	P^+	AP^-	P^-	AP^+
Gd magnetization in GdCo	←	←	→	→
Co magnetization in GdCo	→	→	←	←
FM magnetization	→	←	←	→

Fig. 2(a) compares the magnetic configurations adopted by the four spin valves after being irradiated by one, two (up to four consecutive) femtosecond laser pump pulse(s) with an injected fluence fixed to F=16 mJ×cm^{-2}, in the absence of any external magnetic field. The term "injected fluence" refers to the energy per unit area delivered by an ultrafast laser pulse incident on the sample surface (capping layer side). All spin valves were initialized in a P^+ configuration using an external magnetic field. The irradiation by a few laser pulses induces the transition from dark red (P^+) to light blue (AP^-) in the MOKE images, i.e., the full reversal of the FM magnetization while the magnetization of the Co/$Gd_{33}Co_{67}$ bilayer is unaltered, for all spin valves except the one using $Co_{10}Ni_{90}$. Performing the same experiments without the Co/$Gd_{33}Co_{67}$ layer leads to a multidomain state for all FM layers (see Suppl. Mater. Section S1 for an example using $Co_{20}Ni_{80}$) [31]. Moreover, conducting the same experiments but starting from the AP^- configuration yields no effect on the FM magnetic configuration. Consequently, we can conclude that the reversal of the FM layer in our in-plane magnetized spin valve can be attributed to a spin current pulse originating from the laser-induced Gd demagnetization [23] and whose polarization is antiparallel to the initial magnetization of the FM layer, which flows into and interacts with the FM layer. This explanation is supported by previous studies conducted on a similar spin valve structure exhibiting perpendicular magnetic anisotropy [4,15,22,24,25]. No switching is expected starting in the AP^- state since the Gd-induced spin current is polarized parallel to the FM magnetization.

As already previously discussed, the transition from P^+ state to a uniform AP^- state requires multiple laser pulses for the spin valves using $Co_{20}Ni_{80}$, $Co_{40}Ni_{60}$, and CoFeB. Notably, this is the first report of multiple laser pulses inducing magnetization switching in a spin valve structure. As shown in Suppl. Mater. Section S2 this does not depend on the laser pulse fluence

[31]. The first single pulse only partially modifies the P^+ state, and the MOKE image after the pulse shows a non-uniform magnetic contrast, the so-called Partial AP^- state (Fig. 2(a)). It must be composed of P^+ and AP^- domains whose size is smaller than our MOKE microscope resolution so that the MOKE signal averages the contrasts of P^+ and AP^- regions weighted by their relative area. Fig. 2(b), 2(c), and 2(d) present the corresponding magnetic contrast as a function of position along the radius of the circular irradiated region. It is interesting to note that the degree of partial switching, i.e., the MOKE signal value, in the Partial AP^- state after the first pulse varies for different FM layers. The Partial AP^- state closest to the AP^- state occurs in the case of FM=$Co_{20}Ni_{80}$. Moreover, upon exposing the sample to a second pulse, only the spin valve with FM=$Co_{20}Ni_{80}$ reaches a uniform AP^- state (see Fig. 2(d) and the uniform light blue round-shaped domain in Fig. 2(a)), while the spin valves with $Co_{40}Ni_{60}$ and CoFeB require a third laser pulse. Subsequent pulses do not alter the AP^- configuration but result in an expansion of the switched domain size. A more quantitative analysis of the Kerr contrast change as a function of the switched domain size after each pulse excitation is depicted in Suppl. Mater. Section S3 [31]. Finally, it was observed that the threshold pulse fluence required for full reversal increases as the T_C of the FM layer deviates from that of GdCo. This is evidenced by the reduction in the maximum size of the switched area as the T_C of the FM layer increases (as indicated by the 3rd pulse in Fig. 2(a)). This observation is consistent with findings reported in the context of all-optical helicity-independent switching in single GdCo alloys [21]. The comparison among the four studied spin valves having FM layers with various T_C reveals that the switching of the FM layer can only be achieved for FM having a T_C larger than the one of the GdCo spin current emitter. Indeed, in the case of FM=$Co_{10}Ni_{90}$, full reversal is never achieved, and the layer remains multidomain, regardless of the number of pulses applied. Moreover, if the T_C (FM) > T_C (GdCo) condition is fulfilled, increasing the FM layer T_C further from that of GdCo makes the switching more challenging to obtain.

To summarize this section, our careful analysis demonstrates that reversing the FM layer with multiple pulses, even as thin as 3 nm, suggests the presence of a cumulative effect, indicating that the layer preserves the memory of previous pulses. This observation is seen for both CoFeB and CoNi FM layers. In addition, the result implies that the angular momentum provided by a single pulse might be insufficient for full reversal, requiring the angular momentum transfer from several pulses. As a result, it raises the question of whether reducing the thickness of the FM layer could potentially minimize the number of pulses needed for full reversal.

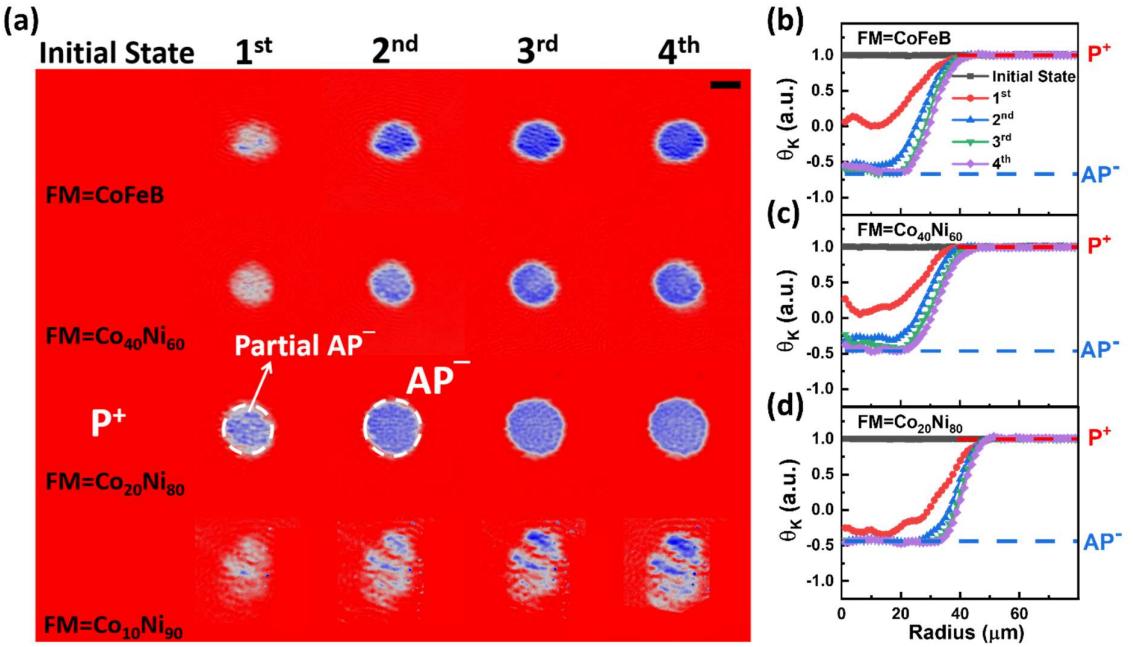

FIG. 2. All-optical switching for in-plane magnetized Co (3 nm)/Gd-rich $Gd_{33}Co_{67}$ (5 nm)/Cu (10 nm)/an FM layer (3 nm) spin valves. (a) Longitudinal Kerr images after irradiating the spin valves with one, two, three, and four femtosecond single pulse, with a fixed laser fluence of F=16 mJ×cm^{-2}, starting from an initial P^+ configuration. The scale bar in the Kerr images is 100 μm long. The obtained magnetic contrast as a function of the position along the radius of the circular irradiated region, with zero denoting the center, for spin valves with FM layers of (b) CoFeB, (c) $Co_{40}Ni_{60}$, and (d) $Co_{20}Ni_{80}$, respectively.

C. Variation of the ferromagnetic layers thickness with a fixed Curie temperature

We now focus on the influence of the FM thickness on the magnetization switching by a spin current generated by the GdCo demagnetization in an in-plane magnetized spin valve. For this purpose, we use the second series of spin valve structures: Glass/Ta (3 nm)/$Gd_{25}Co_{75}$ (5 nm)/Cu (5 nm)/$Co_{40}Fe_{40}B_{20}$ (t nm)/Pt (3 nm), where t varies from 1 to 2.45 nm and the $Gd_{25}Co_{75}$ alloy is a Gd-dominant sample. As shown in Fig. 3(a) and 3(b), the CoFeB layer thickness does not affect neither the room temperature saturation magnetization (M_S), which remains around 1030±50 kA/m, nor the T_C, which is approximately 680 K. The temperature dependence of M_S for various CoFeB layers (t nm) and the corresponding fit are shown in Suppl. Mater. Section S4 [31]. Such invariance likely originates from the amorphous nature of the CoFeB. Note that, for comparison, the M_S of the $Gd_{25}Co_{75}$ layer is around 270±50 kA/m, and its T_C is estimated from previous reports to be approximately 720 K [27,28]. Furthermore, as presented in Suppl. Mater. Section S5, the longitudinal MOKE hysteresis loops for structures containing $Gd_{25}Co_{75}$ (5 nm)/Cu (5 nm)/CoFeB (t nm) exhibit a square-shaped profile, depicting four distinct

magnetic configurations for all samples: P^+, AP^-, P^-, and AP^+ (as defined in the previous section) [31].

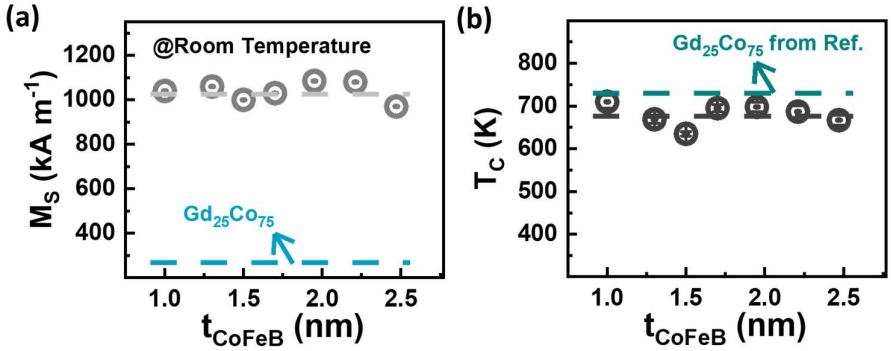

FIG. 3. Magnetic properties of Gd-rich $Gd_{25}Co_{75}$ (5 nm)/Cu (5 nm)/CoFeB (t nm) in-plane magnetized spin valve structures. (a) The CoFeB saturation magnetization (M_S) measured at room temperature as a function of the CoFeB layer thickness (t), the light gray dashed line serves as a guide to the eye, and the blue dashed line shows the room temperature M_S of the $Gd_{25}Co_{75}$. (c) Curie temperature (T_C) as a function of t, with a dark cyan dashed line indicating the T_C of the $Gd_{25}Co_{75}$ alloy, obtained from references [27,28], and a dark gray dashed line providing a visual reference for the T_C of CoFeB layers.

Fig. 4(a) summarizes the MOKE images measured after irradiating the spin valves with successive single laser pulses with fluences ranging between 8 and 11 mJ×cm^{-2}. Starting from the P^+ configuration, three distinct Kerr contrast changes are observed depending on the CoFeB layer thickness. For the thinner CoFeB layers with thicknesses of 1.5, 1.7, and 1.95 nm, a full single pulse switching of the CoFeB is observed. Indeed, the first single laser pulse initiates a transition from dark red (P^+) to a circular dark blue (P^-) region, surrounded by a light red ring (AP^+). The co-existence of these two final states is due to the Gaussian energy radial profile of the laser pulse, which has a maximum at the center of the laser spot and decreases as the distance with the center increases. The transition from P^+ to AP^+ in the outer ring region of the irradiated area indicates the all-optical helicity-independent switching (AO-HIS) of the GdCo layer magnetization alone [21]. In contrast, the central region undergoes a transition from P^+ to P^-, during which both GdCo and CoFeB magnetizations fully reverse after the first single pulse. Upon exposure to the second pulse, both the inner and outer regions switch back to the P^+ state. These observations can be successively reproduced with every odd and even number of laser pulses. As observed in various perpendicularly magnetized systems, the full reversal of the ferromagnetic layer (CoFeB) is induced by a single laser pulse, leading to the ultrafast GdCo demagnetization and, consequently, an angular momentum transfer to the FM layer [4,15,22,24,25]. Similar experiments, as shown in Suppl. Mater. Section S6, starting from the AP^+ configuration, demonstrates that only the magnetization of the GdCo layer reverses after

the first pulse [31]. However, for the second pulse, the magnetization of the GdCo layer switches back, and the reversal of the CoFeB's magnetization occurs in a smaller region.

To confirm the effectiveness of the spin transport interpretation for explaining the switching of the CoFeB magnetization, we fabricated a spin valve incorporating an insulating MgO layer within the Cu spacer. As described in Suppl. Mater. Section S7, our experiments demonstrated that the full CoFeB reversal occurs in the absence of the MgO layer, whereas the addition of the MgO layer results in only a demagnetized state of the CoFeB layer [31]. The results indicate that the MgO layer blocks the spin currents from the Gd sublattice, thereby preventing their interaction with the CoFeB magnetization. As a result, this inhibition leads to the absence of switching in the CoFeB layer and only results in forming a multidomain state. Additionally, our findings reveal that the full switching of the CoFeB layer is consistently observed, exhibiting identical switching behavior regardless of the polarization of the laser pulse, whether linear or circularly polarized.

Increasing the thickness of the FM layer does not impact the GdCo switching of the outer region, as the switching mechanism solely relies on the ultrafast demagnetization of GdCo itself. However, the radius of the P^- region decreases with increasing t. For t values above 2.2 nm, the MOKE contrast at the center of the irradiated region no longer indicates an entirely uniform P^- state. Instead, it shows a transition in the CoFeB switching behavior: from full reversal to partial switching (observed as a light blue color for t=2.2 nm) and ultimately to hardly partial reversal (noted as a mixture of randomly distributed red and blue for t=2.45 nm). In Fig. 4(b), the variation in magnetization of the CoFeB layer after the first single pulse, calculated from the MOKE signal in the central region, is plotted against increasing CoFeB thickness. Single pulse-induced full deterministic reversal of the CoFeB layer can only be achieved up to approximately t=2 nm when using a $Gd_{25}Co_{75}$ (5 nm) layer as the spin current source.

To summarize the observed switching behaviors in the second series of spin valves with the $Gd_{25}Co_{75}$ layer, Fig. 4(c) shows the injected threshold fluences (F^{th}) required to obtain different magnetic configurations, plotted as a function of the thickness of the CoFeB layer. These configurations include the fluence required to switch the $Gd_{25}Co_{75}$ magnetization ($F^{th}_{P^+\rightarrow AP^+}$), as well as the fluences needed for achieving full and partial reversal of the CoFeB magnetization ($F^{th}_{P^+\rightarrow P^-}$ and $F^{th}_{P^+\rightarrow Partial\ P^-}$, respectively). The threshold fluence $F^{th}_{P^+\rightarrow AP^+}$ shows a slight linear increase as t increases. This can be understood by calculating the light absorption profile through the Transfer Matrix Method, as described in Suppl. Mater. Section S8 [31]. Since the laser pulse is sent from the CoFeB side, the light absorption in the GdCo

layer slightly decreases with increasing t. As a result, $F^{th}_{P^+\rightarrow AP^+}$ needs to be increased to ensure that the GdCo layer absorbs sufficient energy to trigger the switching. On the other hand, the threshold fluence $F^{th}_{P^+\rightarrow P^-}$ exhibits a more pronounced linear increase with t. For CoFeB thicknesses exceeding t=2 nm, only partial switching of CoFeB magnetization is observed ($F^{th}_{P^+\rightarrow Partial\ P^-}$), but the dependence of this transition on t still follows the variation observed for $F^{th}_{P^+\rightarrow P^-}$.

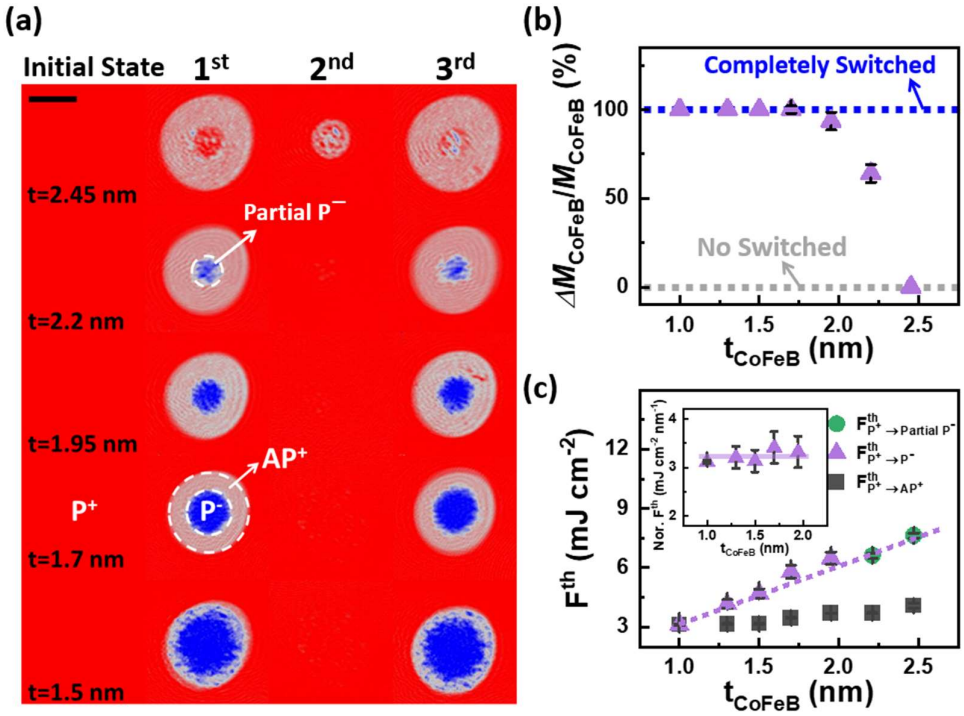

FIG. 4. All-optical switching for the Gd-rich $Gd_{25}Co_{75}$ (5 nm)/Cu (5 nm)/CoFeB (t nm) spin valves with various CoFeB layer thicknesses (t). (a) MOKE images obtained after irradiation with different numbers of laser pulses. The laser fluences used in the measurements range from 8 to 11 mJ×cm^{-2}. The scale bar is 100 μm long. (b) The magnetization changes of CoFeB around the center of the pump pulse spot, estimated from the magnetic contrast changes after the first laser pulse excitation, are plotted as a function of t. Full reversal of the CoFeB layer is indicated by 100%, while 0% represents no reversal of the CoFeB layer. Values between 0% and 100% indicate partial switching of the CoFeB layer. (c) Experimental threshold fluences (F^{th}) for observing various magnetic configurations, starting from the P^+ initial state: fully reversing the GdCo magnetization only ($F^{th}_{P^+\rightarrow AP^+}$, black square symbols), fully reversing the magnetization of both the GdCo and CoFeB layers ($F^{th}_{P^+\rightarrow P^-}$, purple triangle symbols), and fully reversing the GdCo magnetization while partially reversing the CoFeB magnetization ($F^{th}_{P^+\rightarrow Partial\ P^-}$, green circle symbols). These F^{th} values are plotted against t. The purple dashed line is generated by multiplying the obtained $F^{th}_{P^+\rightarrow P^-}$ value at t=1 nm by different t values. The inset shows the corresponding normalized $F^{th}_{P^+\rightarrow P^-}$ values for various t values of the CoFeB layer.

The inset in Fig. 4(c) exhibits the normalized $F^{th}_{P^+\rightarrow P^-}$ values of the second series of spin valves using the $Gd_{25}Co_{75}$ as spin current source, where all measured $F^{th}_{P^+\rightarrow P^-}$ values were normalized by the corresponding film thickness. Notably, these normalized $F^{th}_{P^+\rightarrow P^-}$ values remain constant despite increasing the t value of the CoFeB layer. Since the T_C of CoFeB remains constant regardless of its thickness, the results presented in Fig. 4(c) indicate that the increase in the threshold to reverse CoFeB is directly associated with its thickness (or volume).

Next, we study the impact of the available spin current entering the CoFeB layer, thereby affecting the single-pulse P^+ to P^- switching. This can be verified by adjusting the amount of Gd in the GdCo layer [23]. In the case of $Gd_{25}Co_{75}$ (as shown in Fig. 4), the threshold thickness of CoFeB is found to be t=2 nm. We performed the all-optical switching measurements on the second series of spin valves consisting of Glass/Ta (3 nm)/Co-rich $Gd_{17.5}Co_{82.5}$ (5 nm)/Cu (5 nm)/CoFeB (t nm)/Pt (3 nm) as shown in Fig. 5. Fig. 5(a) shows the data collected with pulse fluences of 6.5 mJ×cm^{-2} and 10 mJ×cm^{-2} for t values of 1.3 and 1.7 nm, respectively. P^+ to P^- switching cannot be achieved for t=1.7 nm; instead, partial CoFeB magnetization switching is observed. However, when t is decreased to t=1.3 nm, a full and uniform P^+ to P^- switched domain is obtained. The three thresholds are evaluated using the method described above and plotted as a function of CoFeB thickness, as shown in Fig. 5(b). The threshold fluence ($F^{th}_{P^+\rightarrow AP^+}$) for AO-HIS of $Gd_{17.5}Co_{82.5}$ exhibits a slight increase as t increases. On the other hand, for t=1.3 nm, the $F^{th}_{P^+\rightarrow P^-}$ value is higher when using $Gd_{17.5}Co_{82.5}$ compared to $Gd_{25}Co_{75}$. The value of $F^{th}_{P^+\rightarrow Partial\ P^-}$ can be determined for t=1.7 nm. We can conclude that for $Gd_{17.5}Co_{82.5}$, the threshold thickness is between 1.3 and 1.7 nm, which is significantly lower than for $Gd_{25}Co_{75}$. As discussed below, it can be explained by the fact that the angular momentum generated by the Gd demagnetization is reduced if the Gd concentration decreases.

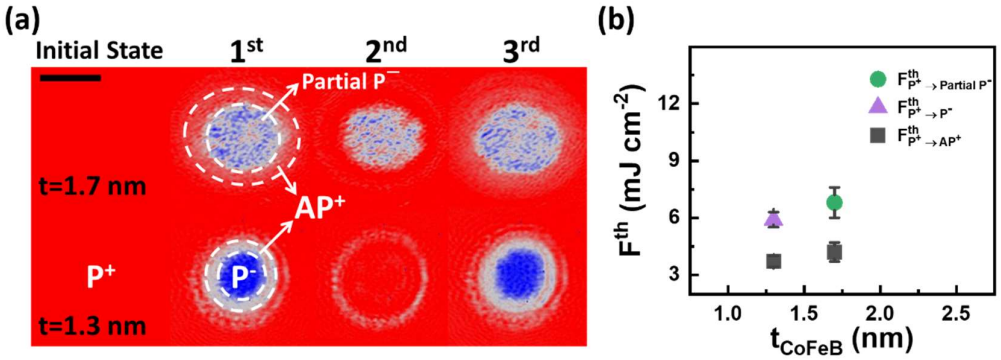

FIG. 5. All-optical switching for Co-rich $Gd_{17.5}Co_{82.5}$ (5 nm)/Cu (5 nm)/CoFeB (t nm) spin valves with t=1.3 and 1.7 nm. (a) MOKE images obtained after irradiation with different numbers of laser pulses. For the case of t=1.3 nm, a laser fluence of 6.5 mJ×cm^{-2} was used, while for t=1.7 nm, a laser fluence of 10 mJ×cm^{-2} was employed. The scale bar in the images is 100 µm long. (b) Experimental threshold fluences (F^{th}) for observing various magnetic configurations, starting from the P^+ initial state: fully reversing the GdCo magnetization only ($F^{th}_{P^+\rightarrow AP^+}$, black square symbols), fully reversing the magnetization of both the GdCo and CoFeB layers ($F^{th}_{P^+\rightarrow P^-}$, purple triangle symbols), and fully reversing the GdCo magnetization while partially reversing the CoFeB magnetization ($F^{th}_{P^+\rightarrow Partial\ P^-}$, green circle symbols). These F^{th} values are plotted against t.

IV. DISCUSSION

We have demonstrated that the impact of the Curie temperature (T_C) and the layer thickness (t) of the ferromagnetic (FM) layer, as well as the GdCo concentration, on the light-induced magnetization reversal of the FM layer, can be disentangled using GdCo/Cu/FM layer in-plane magnetized spin valves. Our study confirms that the upper threshold limit of thickness is significantly influenced by the Gd concentration. The reversal of the FM layer can be explained by the angular momentum transfer generated by the Gd demagnetization spin current pulse to the FM layer's magnetization.

To achieve FM magnetization reversal, the FM's magnetization must undergo a significant reduction (demagnetization) upon the arrival of the current pulse. This demagnetization can occur due to direct laser irradiation and the presence of hot electrons within the spin valve [32]. Our study demonstrates that a higher Curie temperature of the FM results in a larger laser fluence threshold required to significantly demagnetize the FM, as previously shown in perpendicularly magnetized CoNi/Cu/GdFeCo spin valves by Igarashi *et al.* [25]. Additionally, we clearly showed that for a given Curie temperature, the thicker the FM layer, the higher the laser threshold fluence needed. We also observed that beyond a certain thickness, several pulses are required to achieve full magnetization reversal of the FM layer. In

alignment with our understanding, as the thickness of the FM layer increases, more FM magnetic moments need to be demagnetized, and a greater amount of spin current angular momentum from the Gd demagnetization is necessary to affect the entire FM layer. This can be accomplished by increasing the laser pulse fluence, thereby increasing Gd demagnetization or increasing the number of pulses and the Gd concentration of the GdCo alloy. An increase in T_C leads to an elevated threshold fluence required for sufficient demagnetization of CoNi and, consequently, for full magnetization switching. This explains the results depicted in Fig. 2(a) for the samples demonstrating full switching where higher T_C of the FM layer requires a higher switching threshold fluence.

Moreover, FM layers with higher T_C require a larger number of pulses for full reversal, as a higher T_C FM layer experiences a smaller reduction in magnetization per pulse, necessitating more pulses for complete reversal. This cumulative effect indicates that the FM layer does not need to be fully demagnetized for reversal; partial demagnetization followed by successive pulses can achieve the reversal. For low T_C FM layers like $Co_{10}Ni_{90}$, the entire FM layer must be completely demagnetized for a longer period to maintain the angular momentum provided by the Gd current pulse.

In GdCo/Cu/CoFeB spin valves, where single pulse reversal of the CoFeB layer was achieved, T_C remains constant as CoFeB thickness varies. However, a linear variation of switching threshold fluence with thickness was still observed. This trend suggests that as the thickness of the FM layer increases, more magnetic moments need to be demagnetized, requiring a higher amount of spin current from the Gd. This can be achieved by increasing the laser pulse fluence, which enhances Gd demagnetization, thereby increasing the thickness of CoFeB that can be switched.

The findings also indicate that reducing the Gd concentration decreases the upper threshold thickness and increases the threshold fluence needed for full reversal of the FM layer. This is because lower Gd content results in reduced angular momentum transfer from Gd, necessitating higher pulse fluence for sufficient demagnetization of the FM layer.

V. CONCLUSION

Our study demonstrates femtosecond laser pulse-induced magnetization switching of various ferromagnetic (FM) layers within in-plane magnetized GdCo/Cu/FM spin valves by applying Gd current pulses. We examined the influence of the Curie temperature, the thickness of the FM layer, and the Gd concentration in the GdCo alloy. The in-plane magnetization

geometry allows the study of thick FM layers without multi-domain formation due to dipolar fields. In this geometry, we observed a transition from single pulse switching for thin FM layers to multiple pulse switching for thick FM layers.

All measurements confirm our understanding that the reversal of the FM layer occurs when the laser pulse induces sufficient demagnetization across the entire FM layer and sufficient angular momentum transfer from Gd demagnetization. This implies that the Curie temperatures of both the GdCo and the FM layer must be close to each other, and the amount of angular momentum generated increases with the Gd concentration in the GdCo alloy. Conversely, the amount of angular momentum needed for FM magnetization switching decreases with a reduction in the FM layer thickness.

Furthermore, we revealed that the upper threshold thickness is determined by the amount of spin current. With a GdCo layer featuring a higher Gd concentration, we could reverse a relatively thick FM layer using multiple pulses. Our findings show a transition from multiple to single pulse-induced magnetization reversal, shedding light on the intrinsic all-optical switching mechanism where the total angular momentum transferred to the entire FM layer is a key parameter for magnetization manipulation. This study offers insights for designing energy-efficient magnetic memory devices and proposes a geometric configuration for understanding FM layer reversal induced by spin currents using Terahertz time-domain spectroscopy.

ACKNOWLEDGMENTS

This work is supported by the ANR-20-CE09-0013 UFO, ANR-20-CE24-0003 SPOTZ and ANR SLAM, the Institute Carnot ICEEL, the Région Grand Est, the Metropole Grand Nancy for the project “OPTIMAG” and FASTNESS, the interdisciplinary project LUE “MAT-PULSE”, part of the French PIA project “Lorraine Université d’Excellence” reference ANR-15-IDEX-04-LUE, a European Union Program, the European Union’s Horizon 2020 research and innovation program COMRAD under the Marie Skłodowska-Curie grant agreement No 861300. This article is based upon work from COST Action CA17123 MAGNETOFON, supported by COST (European Cooperation in Science and Technology). This work was supported by the ANR through the France 2030 government grants EMCOM (ANR-22-PEEL-0009), PEPR SPIN (ANR-22-EXSP 0002) and PEPR SPIN – SPINMAT ANR-22-EXSP-0007. All funding was shared equally among all authors.

References

1. J.-Y. Chen, L. He, J.-P. Wang, and M. Li, All-Optical Switching of Magnetic Tunnel Junctions with Single Subpicosecond Laser Pulses, Phys. Rev. Applied **7**, 021001 (2017).
2. A. V. Kimel, and M. Li, Writing magnetic memory with ultrashort light pulses, Nat. Rev. Mater. **4**, 189 (2019).
3. D. Salomoni, Y. Peng, L. Farcis, S. Auffret, M. Hehn, G. Malinowski, S. Mangin, B. Dieny, L. D. Buda-Prejbeanu, R. C. Sousa, and I. L. Prejbeanu, Field-Free All-Optical Switching and Electrical Readout of Tb/Co-Based Magnetic Tunnel Junctions, Phys. Rev. Applied **20**, 034070 (2023).
4. Q. Remy, J. Hohlfeld, M. Vergès, Y. Le Guen, J. Gorchon, G. Malinowski, S. Mangin, and M. Hehn, Accelerating ultrafast magnetization reversal by non-local spin transfer, Nat. Commun. **14**, 445 (2023).
5. E. Beaurepaire, J.-C. Merle, A. Daunois, and J.-Y. Bigot, Ultrafast Spin Dynamics in Ferromagnetic Nickel, Phys. Rev. Lett. **76**, 4250 (1996).
6. M. Battiato, K. Carva, and P. M. Oppeneer, Superdiffusive Spin Transport as a Mechanism of Ultrafast Demagnetization, Phys. Rev. Lett. **105**, 027203 (2010).
7. M. Beens, R. A. Duine, and B. Koopmans, s−d model for local and nonlocal spin dynamics in laser-excited magnetic heterostructures, Phys. Rev. B **102**, 054442 (2020).
8. M. Beens, K. A. de Mare, R. A. Duine, and B. Koopmans, Spin-polarized hot electron transport versus spin pumping mediated by local heating, J. Phys.: Condens. Matter **35**, 035803 (2023).
9. B. Liu, H. Xiao, and M. Weinelt, Microscopic insights to spin transport–driven ultrafast magnetization dynamics in a Gd/Fe bilayer, Sci. Adv. **9**, eade0286 (2023).
10. G. Malinowski, F. Dalla Longa, J. H. H. Rietjens, P. V. Paluskar, R. Huijink, H. J. M. Swagten, and B. Koopmans, Control of speed and efficiency of ultrafast demagnetization by direct transfer of spin angular momentum, Nature Phys. **4**, 855 (2008).
11. D. Rudolf, C. La-O-Vorakiat, M. Battiato, R. Adam, J. M. Shaw, E. Turgut, P. Maldonado, S. Mathias, P. Grychtol, H. T. Nembach, T. J. Silva, M. Aeschlimann, H. C. Kapteyn, M. M. Murnane, C. M. Schneider, and P. M. Oppeneer, Ultrafast magnetization enhancement in metallic multilayers driven by superdiffusive spin current, Nat. Commun. **3**, 1037 (2012).
12. G.-M. Choi, B.-C. Min, K.-J. Lee, and D. G. Cahill, Spin current generated by thermally driven ultrafast demagnetization, Nat. Commun. **5**, 4334 (2014).
13. G.-M. Choi, C.-H. Moon, B.-C. Min, K.-J. Lee, and D. G. Cahill, Thermal spin-transfer torque driven by the spin-dependent Seebeck effect in metallic spin-valves, Nature Phys. **11**, 576 (2015).
14. Y. L. W. van Hees, P. van de Meugheuvel, B. Koopmans, and R. Lavrijsen, Deterministic all-optical magnetization writing facilitated by non-local transfer of spin angular momentum, Nat. Commun. **11**, 3835 (2020).
15. X. Fan, M. Hehn, G. Wei, G. Malinowski, T. Huang, Y. Xu, B. Zhang, W. Zhang, X. Lin, W. Zhao, and S. Mangin, On/Off Ultra-Short Spin Current for Single Pulse Magnetization Reversal in a Magnetic Memory Using VO_2 Phase Transition, Adv. Electron. Mater. **8**, 2200114 (2022).
16. J. Igarashi, W. Zhang, Q. Remy, E. Díaz, J.-X. Lin, J. Hohlfeld, M. Hehn, S. Mangin, J. Gorchon, and G. Malinowski, Optically induced ultrafast magnetization switching in ferromagnetic spin valves, Nat. Mater. **22**, 725 (2023).

17. I. Radu, K. Vahaplar, C. Stamm, T. Kachel, N. Pontius, H. A. Dürr, T. A. Ostler, J. Barker, R. F. L. Evans, R. W. Chantrell, A. Tsukamoto, A. Itoh, A. Kirilyuk, T. Rasing, and A. V. Kimel, Transient ferromagnetic-like state mediating ultrafast reversal of antiferromagnetically coupled spins, Nature **472**, 205 (2011).
18. T. A. Ostler, J. Barker, R. F. L. Evans, R. W. Chantrell, U. Atxitia, O. Chubykalo-Fesenko, S. El Moussaoui, L. Le Guyader, E. Mengotti, L. J. Heyderman, F. Nolting, A. Tsukamoto, A. Itoh, D. Afanasiev, B. A. Ivanov, A. M. Kalashnikova, K. Vahaplar, J. Mentink, A. Kirilyuk, T. Rasing, and A.V. Kimel, Ultrafast heating as a sufficient stimulus for magnetization reversal in a ferrimagnet, Nat. Commun. **3**, 666 (2012).
19. M. L. M. Lalieu, M. J. G. Peeters, S. R. R. Haenen, R. Lavrijsen, and B. Koopmans, Deterministic all-optical switching of synthetic ferrimagnets using single femtosecond laser pulses. Phys. Rev. B **96**, 220411(R) (2017).
20. C. Banerjee, N. Teichert, K. E. Siewierska, Z. Gercsi, G. Y. P. Atcheson, P. Stamenov, K. Rode, J. M. D. Coey, and J. Besbas, Single pulse all-optical toggle switching of magnetization without gadolinium in the ferrimagnet Mn_2Ru_xGa, Nat. Commun. **11**, 4444 (2020).
21. J.-X. Lin, M. Hehn, T. Hauet, Y. Peng, J. Igarashi, Y. Le Guen, Q. Remy, J. Gorchon, G. Malinowski, S. Mangin, and J. Hohlfeld, Single Laser Pulse Induced Magnetization Switching in In-Plane Magnetized GdCo alloys, Phys. Rev. B **108**, L220403 (2023).
22. S. Iihama, Y. Xu, M. Deb, G. Malinowski, M. Hehn, J. Gorchon, E. E. Fullerton, and S. Mangin, Single-shot multi-level all-optical magnetization switching mediated by spin transport, Adv. Mater. **30**, 1804004 (2018).
23. G.-M. Choi, and B.-C. Min, Laser-driven spin generation in the conduction bands of ferrimagnetic metals. Phys. Rev. B **97**, 014410 (2018).
24. Q. Remy, J. Igarashi, S. Iihama, G. Malinowski, M. Hehn, J. Gorchon, J. Hohlfeld, S. Fukami, H. Ohno, and S. Mangin, Energy efficient control of ultrafast spin current to induce single femtosecond pulse switching of a ferromagnet, Adv. Sci. **7**, 2001996 (2020).
25. J. Igarashi, Q. Remy, S. Iihama, G. Malinowski, M. Hehn, J. Gorchon, J. Hohlfeld, S. Fukami, H. Ohno, and S. Mangin, Engineering Single-Shot All-Optical Switching of Ferromagnetic Materials, Nano Lett. **20**, 8654 (2020).
26. T. Lichtenberg, Y. L. W. van Hees, M. Beens, C. J. Levels, R. Lavrijsen, R. A. Duine, and B. Koopmans, Probing laser-induced spin-current generation in synthetic ferrimagnets using spin waves, Phys. Rev. B **106**, 094436 (2022).
27. P. Hansen, C. Clausen, G. Much, M. Rosenkranz, and K. Witter, Magnetic and magneto-optical properties of rare-earth transition-metal alloys containing Gd, Tb, Fe, Co, J. Appl. Phys. **66**, 756 (1989).
28. N. H. Duc, and D. Givord, Exchange interactions in amorphous GdCo alloys, J. Magn. Magn. Mater. **157**, 169 (1996).
29. K. J. Harte, Theory of Magnetization Ripple in Ferromagnetic Films, J. Appl. Phys. **39**, 1503 (1968).
30. M. Mohanta, S. K. Parida, A. Sahoo, Z. Hussain, M. Gupta, V. R. Reddy, and V. R. R. Medicherla, Structural and magnetic properties of CoNi surface alloys, Physica B: Condensed Matter, **572**, 105 (2019).
31. See Supplemental Material at [URL] for (i) AOS of in-plane magnetized $Co_{20}Ni_{80}$ single layer without the $Co/Gd_{33}Co_{67}$ layer. (ii) Laser pulse fluence-dependent AOS measurements on Co (3 nm)/$Gd_{33}Co_{67}$ (5 nm)/Cu (10 nm)/$Co_{20}Ni_{80}$ (3 nm) spin valve. (iii) Laser pulse fluence-dependent switched domain size for different Co (3 nm)/$Gd_{33}Co_{67}$ (5 nm)/Cu (10 nm)/FM layer (3 nm) spin valves. (iv) Temperature dependence of saturation magnetization and the corresponding fit for CoFeB layers with

different thicknesses. (v) Longitudinal MOKE hysteresis loops of in-plane magnetized $Gd_{25}Co_{75}$ (5 nm)/Cu (5 nm)/CoFeB (t nm) spin valves. (vi) AOS of $Gd_{25}Co_{75}$ (5 nm)/Cu (5 nm)/CoFeB (t nm) spin valves starting from AP^{+} configuration. (vii) Effect of insulator MgO insertion and laser pulse helicity on the single pulse reversal of CoFeB layer. (viii) Absorption profile calculation with different CoFeB thickness. The Supplemental Material also contains Refs. [4,22,24,25,33,34].

32. N. Bergeard, M. Hehn, S. Mangin, G. Lengaigne, F. Montaigne, M. L. M. Lalieu, B. Koopmans, and G. Malinowski, Phys. Rev. Lett. **117**, 147203 (2016).
33. E. Callen, and H. Callen, Ferromagnetic Transitions and the One-Third-Power Law, J. Appl. Phys. **36**, 1140 (1965).
34. X. Liang, X. Xu, R. Zheng, Z. A. Lum, and J. Qiu, Optical constant of CoFeB thin film measured with the interference enhancement method, Appl. Opt. **54**, 1557 (2015).